Artificial Neural Network for Modeling the Tensile Properties of Ferrite-Pearlite Steels: Relative Importance of Alloying Elements and Microstructural Factors

Tae-Woon Hong[1] · **Sang-In Lee**[1] · **Jae-Hyeok Shim**[2] · **Myoung-Gyu Lee**[3] · **Joonho Lee**[4] · **Byoungchul Hwang**[1]

Abstract

An artificial neural network (ANN) model was developed to predict the tensile properties as a function of alloying element and microstructural factor of ferrite-pearlite steels. The input parameters of the model were composed of alloying elements (Mn, Si, Al, Nb, Ti, and V) and microstructural factors (pearlite fraction, ferrite grain size, interlamellar spacing, and cementite thickness), while the output parameters of the model were yield strength and tensile strength. Although the ferrite-pearlite steels have complex relationships among the alloying elements, microstructural factors, and tensile properties, the ANN model predictions were found to be more accurate with experimental results than the existing equation model. In the present study the individual effect of input parameters on the tensile properties was quantitatively estimated with the help of the average index of the relative importance for alloying elements as well as microstructural factors. The ANN model attempted from the metallurgical points of view is expected to be useful for designing new steels having required mechanical properties.

1 Introduction

Over the past decades, ferrite-pearlite steels with their advantages of low cost and simple manufacturing have been widely used for various industries [1–12]. The tensile properties of ferrite-pearlite steels are mainly affected by a number of alloying elements and microstructural factors [13–21]. For ferrite-pearlite steels with carbon content below

✉ Joonho Lee
joonholee@korea.ac.kr

✉ Byoungchul Hwang
bhwang@seoultech.ac.kr

1 Department of Materials Science and Engineering, Seoul National University of Science and Technology, Seoul 01811, Republic of Korea

2 Center for Energy Materials Research, Korea Institute of Science and Technology, Seoul 02792, Republic of Korea

3 Department of Materials Science and Engineering, Seoul National University, Seoul 08826, Republic of Korea

4 Department of Materials Science and Engineering, Korea University, Seoul 02841, Republic of Korea

the eutectoid composition, there are various microstructural factors such as phase fraction, ferrite grain size, interlamellar spacing, and cementite thickness that depend on alloying elements and heat treatment. In addition, the alloying elements that were incorporated to the ferrite-pearlite steels affect the tensile properties thorough solid solution and precipitation strengthening. Because the relationship between alloying elements, microstructural factors, and tensile properties is complex, more systematic studies are necessitated to understand this relationship.

Recently, artificial neural network (ANN) techniques that facilitate the learning of input–output parameter relationship for complex problems have been applied to predict and analyze various phenomena occurring in materials. The main feature of ANNs is that, unlike other analysis methods such as physical models and linear regression models, these do not require a specific equation form and only need sufficient input–output parameter data to solve a problem. ANNs with the capacity for defining the relationship between independent and dependent parameters have been used to elucidate unclear problems and have been successfully applied to numerous applications in materials science [22–25]. ANN models have been reported to design alloys [26] and

to predict microstructures [27], hardness [28], and tensile properties [27] according to chemical compositions and heat treatment conditions in carbon steels with a ferrite-pearlite structure. However, the relative importance of alloying elements and microstructural factors in determining the tensile properties of ferrite-pearlite steels has not been studied yet.

The primary objectives of the present study are: (i) to predict the tensile properties of ferrite-pearlite steels using various alloying elements and microstructural factors, (ii) to determine the influence of alloying elements and microstructural factors on tensile properties individually as well in combinations of two or more input parameters, and (iii) to quantitatively estimate the importance of input parameters on tensile properties by calculating the index of relative importance.

2 Materials and Methodology

2.1 Model Establishment

The experimental data used for this study were collected from published literature [14] on ferrite-pearlite steels with equiaxed grains and a pearlite fraction between 55 and 95%. The data sets consisted of the content of alloying elements such as carbon (C), manganese (Mn), silicon (Si), aluminum (Al), niobium (Nb), vanadium (V), and titanium (Ti) and microstructural factors such as the pearlite fraction (V_P), ferrite grain size (d_F), interlamellar spacing (I_S), and cementite thickness (t_{CM}) with the desired yield strength (YS) and tensile strength (TS). The microstructure of ferrite-pearlite steels was observed using an optical microscope and a field emission scanning electron microscope (FE-SEM; model JSM6700F, JEOL, Japan), then the pearlite fraction, ferrite grain size, and interlamellar spacing were quantitatively measured, as shown in Fig. 1. The cementite thickness was calculated using equation [29].

Sub-size plate-type tensile specimens with a gage length of 25.4 mm were taken along a rolling direction. The tensile tests were performed at room temperature and a strain rate of $3.3 \times 10^{-3}/sec$ using a 10 ton universal testing machine (model; UT-100E, MTDI, Korea) according to the ASTM E8 standard testing method. The input parameters considered for the ANN model development were the C, Mn, Si, Al, Nb, V, and Ti contents, and the pearlite fraction, ferrite grain size, interlamellar spacing and cementite thickness; the

Fig. 1 a Optical and b SEM micrographs showing the microstructural factors (pearlite fraction, ferrite grain size, interlamellar spacing, and cementite thickness) of ferrite-pearlite steels (data set 54)
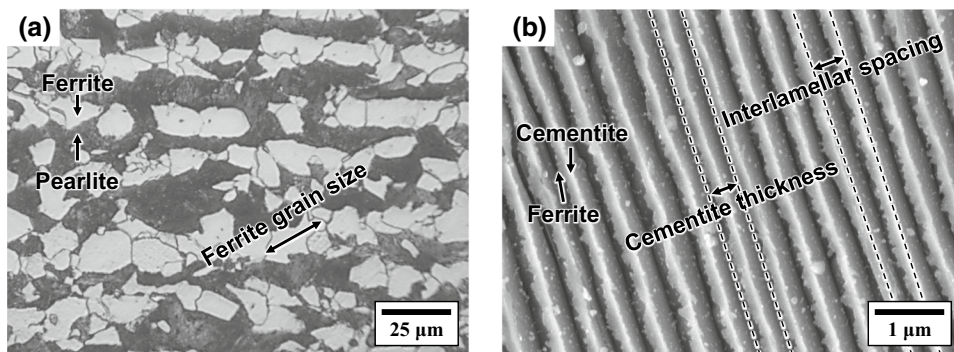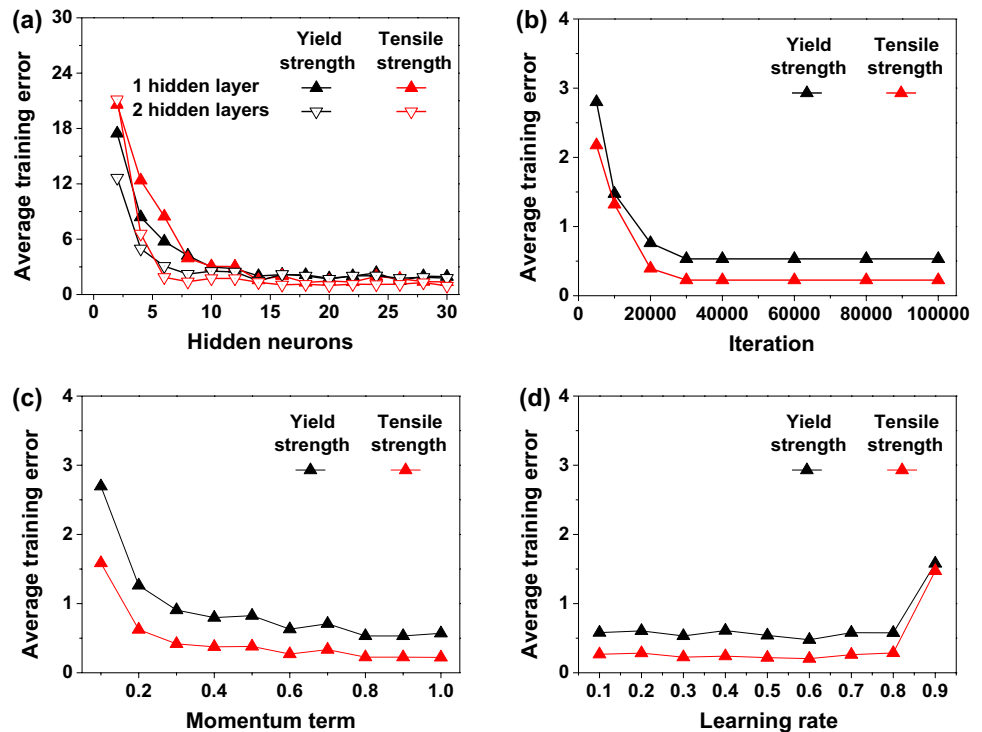
Table 1 Details of the input and output parameters of training and test data used for ANN model

Parameter	Minimum	Maximum	Mean	Standard deviation
Input				
C (wt%)	0.38	0.41	0.39	0.01
Mn (wt%)	0.86	1.54	1.36	0.24
Si (wt%)	0.29	1.04	0.62	0.30
Al (wt%)	0	0.06	0.01	0.02
Nb (wt%)	0	0.05	0.01	0.02
Ti (wt%)	0	0.04	0.01	0.01
V (wt%)	0	0.11	0.01	0.04
Pearlite fraction (vol%)	56.1	92.7	74.5	10.7
Ferrite grain size (μm)	3.5	23.1	8.0	4.5
Interlamellar spacing (μm)	0.210	0.407	0.307	0.05
Cementite thickness (μm)	0.019	0.042	0.027	0.01
Output				
Yield strength (MPa)	321	638	457	73
Tensile strength (MPa)	644	937	774	67

Fig. 2 Variation in average training error as a function of **a** hidden neurons with different hidden layers, **b** iteration, **c** momentum term, and **d** learning rate for yield strength and tensile strength

output parameters were the yield and tensile strength. The details of the input and output parameters used in the study are presented in Table 1. All the paremeters were converted between 0.1 and 0.9. The conversion process is expressed as follows:

$$x_n = \left(\left(x - x_{min} \right) \times 0.8 \right) / \left(x_{max} - x_{min} \right) + 0.1 \qquad (1)$$

where x_n is the converted value of x; x_{max} and x_{min} are the maximum and minimum value of x, respectively, in the entire data sets. Once the best-trained network was found, all the transformed data sets were put back into their original values using the following equation:

$$x = \left(x_n - 0.1 \right) \left(x_{max} - x_{min} \right) / 0.8 + x_{min} \qquad (2)$$

2.2 Modeling Procedure

In this study, the ANN model was trained using a backpropagation algorithm and the sigmoid function was used as an activation function [30, 31]. The ANN model training program and the graphical user interface design of the present ANN model were written in C and Java, respectively. The ANN model consisted of 11 neurons (C, Mn, Si, Al, Nb, V, and Ti contents and pearlite fraction, ferrite grain size, interlamellar spacing, and cementite thickness) in the input layer and two neurons (yield and tensile strength) in the output layer. The neural network training consisted of adjusting

the weights associated with each connection between the neurons until the computed output parameters for each data set of input parameter were as close as possible to the experimental output parameter values. To determine the optimum architecture and to find the confidence of the ANN model, the data sets were split into training and testing data sets. The available 57 data sets were divided into 42 training data sets and 14 testing data sets.

The architecture of the ANN model consists of hidden layers and neurons in the hidden layers, as well as momentum term, learning rate, and number of iterations. The optimal parameters for the network were determined based on the average training error in the output parameter prediction (E_{tr}) of the trained data sets.

$$E_{tr}(y) = \frac{1}{N} \sum_{i=1}^{N} \left| \left(T_i(y) - O_i(y) \right) \right| \qquad (3)$$

where $E_{tr}(y)$ is average training error in the training prediction and testing data sets for output parameter y, N is the number of data sets, $T_i(y)$ is the targeted output parameter, and $O_i(y)$ is the calculated output parameter.

In this study, the momentum term, learning rate, and iterations of the ANN model were optimized as 0.8, 0.3, and 10,000 respectively at the initial state based on the $E_{tr}(y)$. In order to find the suitable number of neurons and hidden layers, two basic structures of the neural networks are examined: one with single hidden layer and the other with two hidden layers. Each structure was train with different hidden

Table 2 Procedure of estimating the index of relative importance (I_{RI}) of input parameters on yield and tensile strength of data set 36

Description of the output properties of the steel

Tensile property	Experimental value (data set 36)	Predicted value (data set 36)	Minimum value (entire data set)	Maximum value (entire data set)	Variation: Maximum-Minimum
Yield strength (MPa)	321	321	321	644	323
Tensile strength (MPa)	666	666	638	937	299

Step by step calculation of I_{RI} for yield and tensile strength

Input parameter description				Yield strength calculation			Tensile strength calculation			Index of relative importance	
Inputs	−3.0 offset	No offset	+3.0 offset	Predicted		Difference	Predicted		Difference	Yield strength (MPa)	Tensile strength (MPa)
				−3.0 offset	+3.0 offset		−3.0 offset	+3.0 offset			
C content (wt%)	0.39	0.40	0.40	318	321	3	683	666	−17	0.004	−0.007
Mn content (wt%)	0.85	0.87	0.89	319	322	3	664	668	4	0.010	0.014
Si content (wt%)	0.34	0.36	0.38	319	323	4	666	666	0	0.012	0.001
Al content (wt%)	−0.00	0	+0.00	323	319	−4	668	664	−4	−0.010	−0.012
Ni content (wt%)	−0.00	0	+0.00	322	320	−2	666	666	0	−0.005	0.002
Ti content (wt%)	−0.00	0	+0.00	321	320	−1	666	666	0	−0.003	−0.002
V content (wt%)	−0.00	0	+0.00	320	322	2	665	667	2	0.007	0.006
Pearlite fraction (vol%)	88.4	89.5	90.6	322	320	−2	667	665	−2	−0.005	−0.008
Ferrite grain size (μm)	22.5	23.1	23.7	322	319	−3	667	665	−2	−0.009	−0.005
Interlamellar spacing (μm)	0.383	0.389	0.395	320	322	−2	665	667	2	0.005	0.006
Cementite thickness (μm)	0.027	0.028	0.029	319	321	3	664	666	2	0.008	0.008

neurons starting from 2 to 20. Figure 2a shows the variation in the average training error as a function of hidden layers and neurons for the yield and tensile strength. The minimum average training error or the output parameters was obtained using two hidden layers with 14 neurons in each layer. The two hidden layers with 14 neuron architecture was selected to optimize the other parameters. The number of iterations executed varied from 5000 to 100,000 as exhibited in Fig. 2b. As the number of iterations increased, the average training errors from the output parameters decreased, and after 30,000 iterations, the average training errors from the output parameters were almost constant. Hence the number of iterations was fixed at 30,000. Once the number of iterations was selected, the momentum term and learning rate coefficients were varied from 0.1 to 0.9 in steps of 0.1, respectively, as provided in Fig. 2c and d. The minimum training errors for the output parameters were generated in a momentum term of 0.8 and a learning rate of 0.6. Therefore, an optimum ANN model with 11–14-14–2 architecture that consisted of an 0.8 momentum term and a 0.6 learning rate with 30,000 iterations was selected in this study. The

optimum ANN model was compared with an existing equation model, as follows [14]:

$$Yield strength \text{ (MPa)} = 15.4\left[V_F^{\frac{1}{3}} \cdot \left(2.3 + 3.8 \cdot (\%Mn) + 1.13 \cdot d_F^{\frac{-1}{2}}\right) \right.$$
$$\left. + \left(1 - V_F^{\frac{1}{3}}\right) \cdot \left(11.6 + 0.25 \cdot I_S^{\frac{-1}{2}}\right) + 4.1 \cdot (\%Si)\right] \tag{4}$$

$$Tensile strength \text{ (MPa)} = 15.4\left[V_F^{\frac{1}{3}} \cdot \left(16.0 + 1.18 \cdot d_F^{\frac{-1}{2}}\right) \right.$$
$$\left. + \left(1 - V_F^{\frac{1}{3}}\right) \cdot \left(46.7 + 0.23 \cdot I_S^{\frac{-1}{2}}\right) + 6.3 \cdot (\%Si)\right] \tag{5}$$

where V_F is the ferrite fraction (vol%), d_F is the ferrite grain size (μm), I_S is the interlamellar spacing (μm), $\%Mn$ is the Mn content (wt%), and $\%Si$ is the Si content (wt%).

2.3 Index of Relative Importance (I_{RI})

The index of relative importance (I_{RI}) is a vector quantity. The direction and amount of the index of relative importance indicate the significance of the input
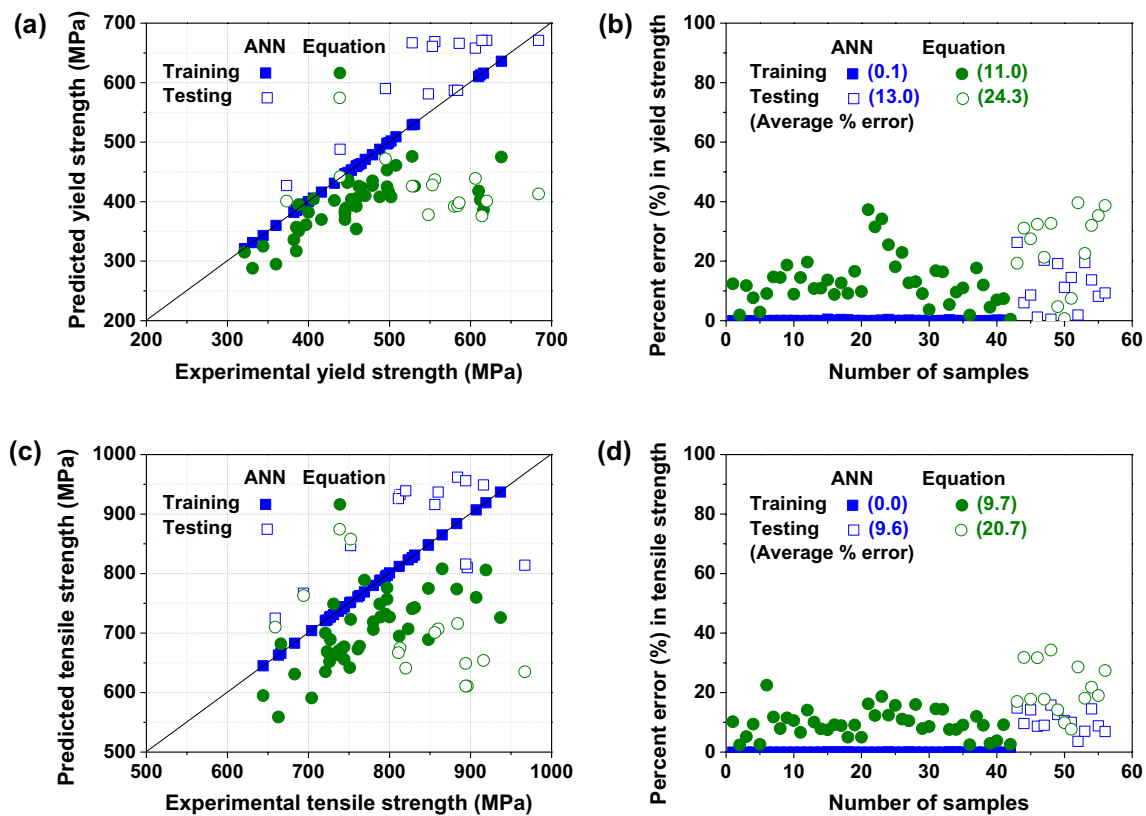
Fig. 3 Performance of the ANN model and the existing equation model [14] for the prediction of the **a** yield strength and **b** tensile strength, and the percent error in the **c** yield strength and **d** tensile strength for 42 training and 14 testing data sets

parameters in the yield and tensile strength. In this study, the instantaneous importance of the input parameters on the output parameters has been estimated. In the equation $Y = f(X_1 + X_2 + X_3 + X_4 \cdots X_{11})$, Y is the yield or tensile strength; X_1 to X_{11}, represent the content of C, Mn, Si, Al, Nb, V, and Ti, and the pearlite fraction, ferrite grain size, interlamellar spacing, and cementite thickness, respectively. The procedure involved the calculation of the index of relative importance as shown below.

(a) The % band of i th input parameter $= ((X_i)Maximum - (X_i)Minimum)/100$
(b) The 6% band of each input parameter was considered i.e., $+3\%$ and -3%
(c) As a result, input parameter X_1 has two row matrices $[+3\% X_1 + X_2 + X_3 + X_4 \cdots X_{11}]$ and $[-3\% X_1 + X_2 + X_3 + X_4 \cdots X_{11}]$
(d) When these two row matrices were passed through the ANN model, $(Y_1)_{+3\%X_1}$ and $(Y_1)_{-3\%X_1}$ were predicted.
(e) The difference, $\Delta(y_1) = (Y_1)_{+3\%X_1} - (Y_1)_{-3\%X_1}$ was calculated.
(f) The index of relative importance (I_{RI}) of input parameter X_1 was calculated from the formula:

$$I_{RI} = \Delta(y_1)/((y_1)Maximum - (y_1)Minimum) \qquad (6)$$

The process (from step 1 to step 6) was repeated to calculate the index of relative importance for the remaining input parameters, and the process for data set 36 is presented in Table 2. While one input parameter was varied by a $\pm 3\%$ offset, the other input parameters were kept constant. After adding the $\pm 3\%$ variation to all the input parameters, ten combinations of input parameter data sets were created. These data sets were fed to the ANN model to predict the respective output parameters and thereby to calculate the index of relative importance for each input parameter.

3 Results and Discussion

The performance of the ANN model can be estimated by calculating the percent error for the output parameter of the testing data set. Figure 3 exhibits the comparison of predictions and percent error in the yield and tensile strength using the ANN model and equation model. For the percent error of the yield and tensile strength (Fig. 3b and d), the ANN model for training data sets has a percent error of 0.1% and
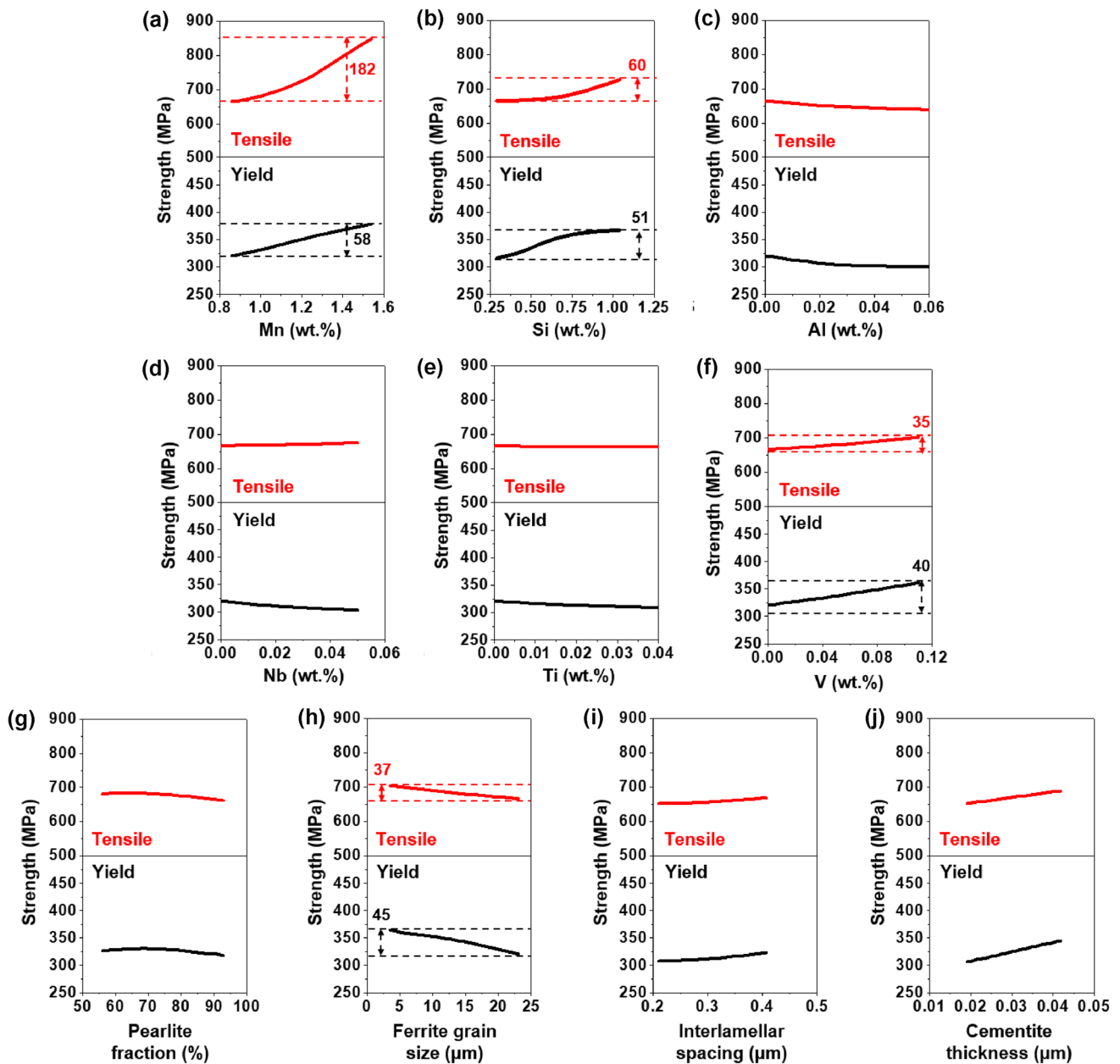
Fig. 4 Predicted yield strength and tensile strength of data set 36 as a function of **a** Mn, **b** Si, **c** Al, **d** Nb, **e** Ti, **f** V contents, **g** pearlite fraction, **h** ferrite grain size, **i** interlamellar spacing and **j** cementite thickness, keeping other input parameters

0.0%, respectively. However, the equation model for training data sets has percent error of 13.0% and 9.6% on the yield and tensile strength, respectively. Even in the yield and tensile strength predictions of testing data sets, percent errors of the ANN model are lower than the equation model with percent errors of 24.3% and 20.7%, respectively, at 11.0% and 9.7%. These results indicate that the ANN model has better agreement with experimental data sets than the equation model. The ANN model that completed the validation can be used to determine the relationships between input parameters and output parameters.

In contrast, most of the carbon in ferrite-pearlite steels is precipitated as carbide and cementite of pearlite [12, 13]. Figure 4 presents the predicted yield and tensile strength of data set 36 as a function of an input parameter except C, keeping other input parameters. The variations in the yield and tensile strength changed more with Mn, Si, and V contents and ferrite grain size compared to the other input parameters. Increasing the Mn, Si, and V contents increases the yield and tensile strength, whereas increasing the ferrite grain size decreases the yield and tensile strength. It is well known that Mn and Si are effective elements for solid
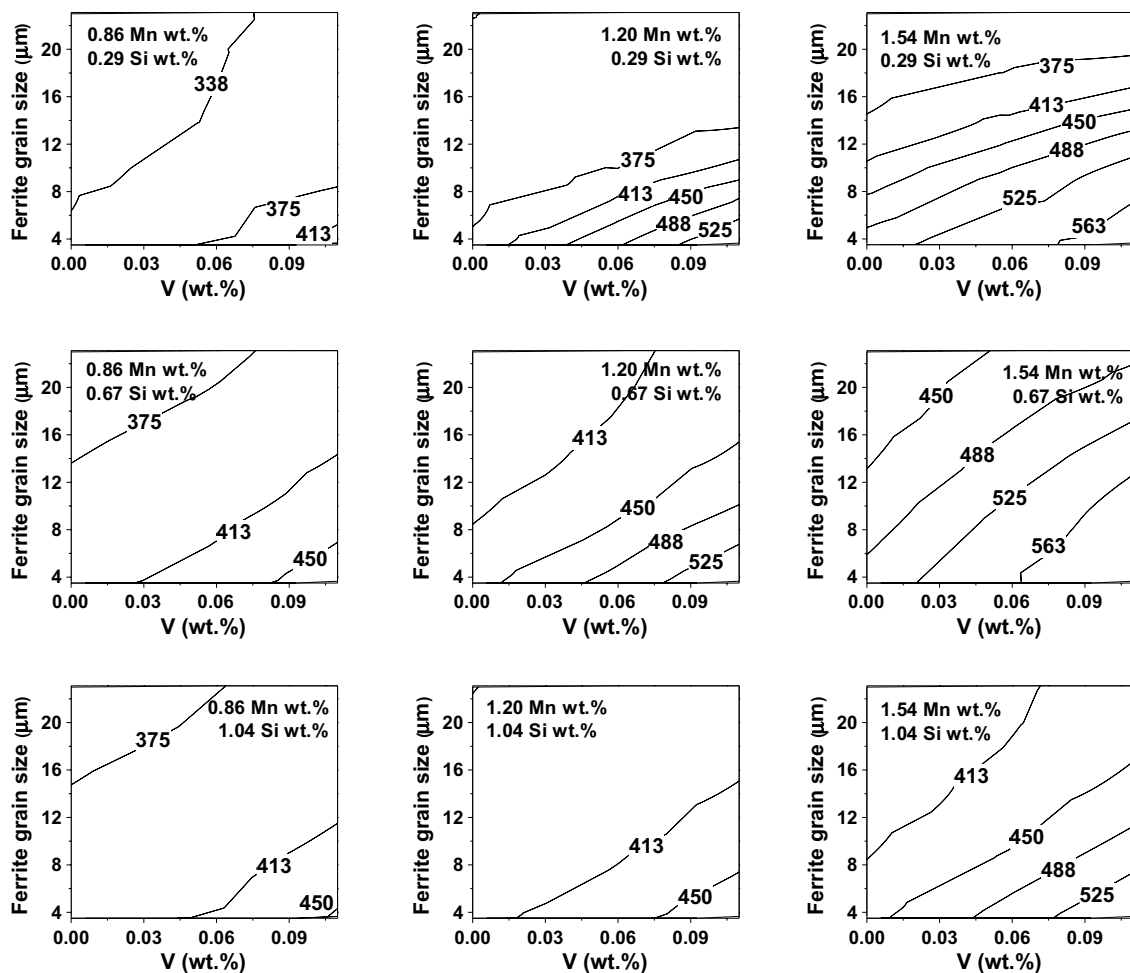
Fig. 5 Contour of predicted yield strength as a function of V content and ferrite grain size at different Si and Mn contents

solution strengthening, and Al, Nb, Ti, and V are stronger elements for precipitation strengthening by forming precipitates such as carbide and nitride combined with C and nitrogen (N) [14–18, 32–37]. Furthermore, it has been reported that the precipitates decrease ferrite grain size and increase ferrite fraction by decreasing austenite grain size due to the pinning effect [32–37]. In the case of microstructural factors, the variations in the yield and tensile strength from each input parameter were mostly similar. The fine interlamellar spacing together fine ferrite grain size commonly increase the yield and tensile strength according to the well-known Hall–Petch relationship [38]. The results in this study indicates that microstructural factors of ferrite-pearlite steels affect the yield and tensile strength by interacting with each other.

Based on the result in Fig. 4, which shows that Mn, Si, and V contents and ferrite grain size substantially change the predicted yield and tensile strength of data set 36, Figs. 5 and 6 exhibit the predicted yield and tensile strength as a function of V content and ferrite grain size for different Mn

and Si contents. The contour plots enable the selection of the condition for the desired yield and tensile strength by visual inspection. The range of Si, Mn and V contents relates to the amount to the usual ferrite-pearlite steels. Each point in Figs. 5 and 6 indicates one ferrite-pearlite steel system. The predicted yield strength tends to increase almost linearly with increasing the content of Mn, Si and V and decreasing ferrite grain size (Fig. 5). At 1.54 wt% Mn and above 0.67 wt% Si, the regions of maximum predicted yield strength are observed for the fine ferrite grain size and high V content. In contrast, the predicted tensile strength increases based only on Mn and Si contents and shows an unclear tendency for V content and ferrite grain size (Fig. 6). The regions of maximum predicted tensile strength are observed at 1.54 wt. Mn and above 0.67 wt% Si. These predicted yield and tensile strength maps will provide an insight into the absolute amounts of alloying elements and microstructural factors needed to make the desired ferrite-pearlite steel that has the required yield and tensile strength.
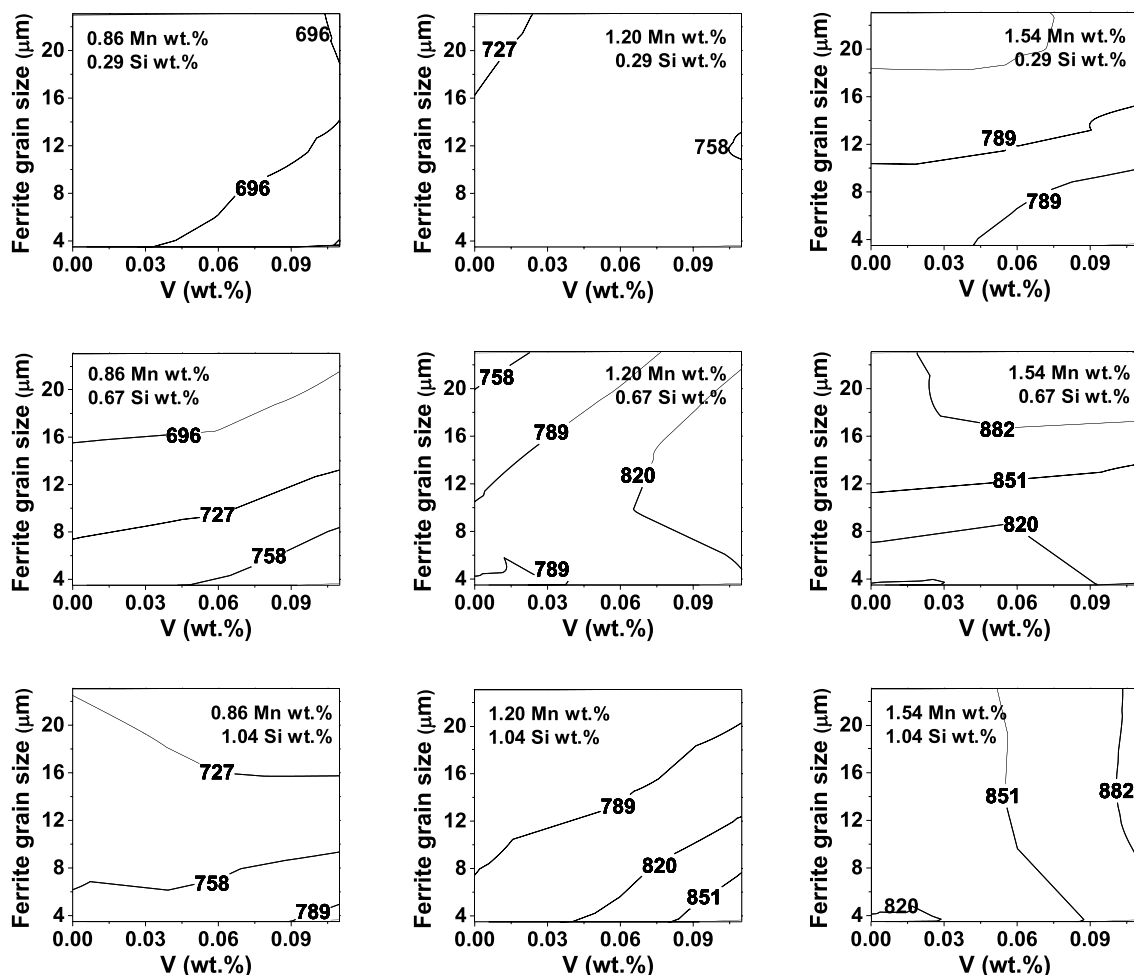
Fig. 6 Contour of predicted tensile strength as a function of V content and ferrite grain size at different Si and Mn contents

There are numbers of reports regarding the effect of various alloying elements and microstructural factors on the yield and tensile strength of ferrite-pearlite steel [3–14]. In this study, to identify the quantitative influence of various alloying elements and microstructural factors, the index of relative importance was calculated. Figure 7 presents the average index of relative importance of the input parameters (alloying elements and microstructural factors) on the output parameters (yield and tensile strength). For the average index of relative importance for yield strength (Fig. 7a), Mn, Si, and V had a positive effect, while the ferrite grain size and interlamellar spacing had a negative effect, and the other input parameters were relatively insignificant. In particular, the V and ferrite grain size had a great effect than other input parameters. The yield strength is generally known to increase when the slip of dislocation is prevented by many factors such as stress field, grain boundary, precipitates, and dislocation [39]. The precipitates and grain boundary are effective inhibitors to the slip of dislocation. Since Al, Nb, and Ti prefer to reduce grain size and V relatively contributes to precipitation strengthening element and,

it is reasonable that the yield strength of ferrite-pearlite steels is greatly influenced by the V content and ferrite grain size.

Figure 7b presents the average index of relative importance of alloying elements and microstructural factors with regard to tensile strength. The Si, V, and pearlite fraction had a positive influence, while the interlamellar spacing had a negative influence, and the influence of other input parameters was minor. In particular, Si and pearlite fraction had the greatest impact. It is well known that tensile strength is related to work hardening after yielding. Precipitates with coherency boundaries with matrix and pearlite are effective at work hardening [40–42]. Furthermore, Si enhances the work hardening of the pearlite and precipitates because the solute Si stabilizes the pearlite and precipitates by diffusing to the interface of the cementite/ferrite and precipitate/ferrite [43–45]. Moreover, the fine interlamellar spacing of pearlite enhances work hardening [40]. Accordingly, it is valid that tensile strength is greatly affected by Si and V contents and pearlite fraction that are related to increasing work hardening.
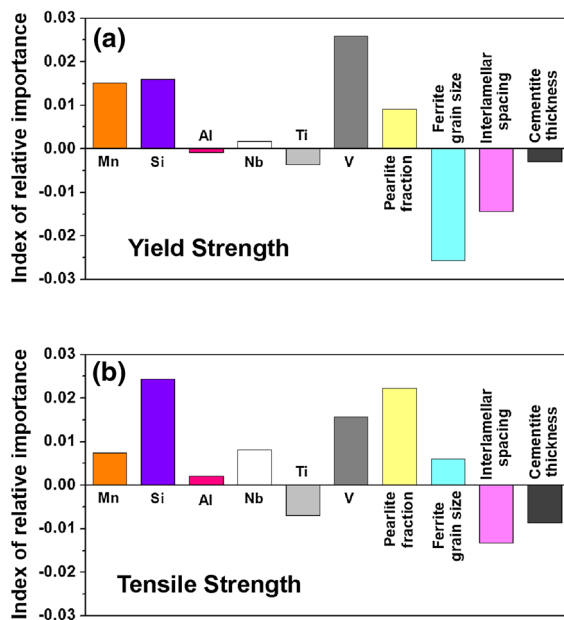
Fig. 7 The average indexes of relative importance of input parameters on the **a** yield strength and **b** tensile strength of ferrite-pearlite steels

4 Conclusions

Based on the present artificial neural network (ANN) analysis for modeling the tensile properties of ferrite-pearlite steels with equiaxed grains, the following conclusions can be drawn.

1. An ANN model has been developed to predict the yield and tensile strength of ferrite-pearlite steels in terms of alloying elements (C, Mn, Si, Al, Nb, Ti, and V) and microstructural factors such as pearlite fraction, ferrite grain size, interlamellar spacing, and cementite thickness.

2. The yield and tensile strength predictions made using the ANN model with unseen data were in good agreement the experimental values, as compared with the calculated properties of the existing model, and the ANN model showed experimentally reliable trends by analyzing the complex nonlinear relationships.

3. The effect of alloying elements and microstructural factors on tensile properties of ferrite-pearlite steels can be quantitatively estimated with the help of the index of relative importance based on the ANN model to understand the complicated effects of input parameters on output parameters.

References

1. N.I. Kim, W. Gil, H.D. Lim, C.H. Choi, H.W. Lee, Met. Mater. Int. **25**, 193–206 (2019)
2. F. Najafkhani, H. Mizadeh, M. Zamani, Met. Mater. Int. **25**, 1039–1046 (2019)
3. S.I. Lee, S.Y. Lee, H.G. Jung, B. Hwang, Met. Mater. Int. **24**, 1221–1231 (2018)
4. H.L. Kim, S.H. Park, Met. Mater. Int. **26**, 14–24 (2020)
5. T. Brlic, S. Reskovic, I. Jandrlic, Met. Mater. Int. **26**, 179–187 (2020)
6. D. Choi, H. Lee, S.K. Cho, H.C. Kim, S.K. Shin, Met. Mater. Int. **26**, 867–881 (2020)
7. H.Y. Lee, Met. Mater. Int. **26**, 1749–1756 (2020)
8. H.L. Kim, S.H. Bang, J.M. Choi, N.H. Tak, S.W. Lee, S.H. Park, Met. Mater. Int. **26**, 1757–1765 (2020)
9. S.I. Lee, J.Y. Kang, S.Y. Lee, B. Hwang, J. Korean Soc. Heat Treat. **29**, 8–14 (2016)
10. S.Y. Lee, S.I. Lee, B. Hwang, Mater Sci. Eng. A **711**, 22–28 (2018)
11. J.H. Shim, B. Hwang, M.G. Lee, J. Lee, Calphad **62**, 67–74 (2018)
12. G. Miyamoto, Y. Karube, T. Furuhara, Acta Mater. **103**, 370–381 (2016)
13. F.B. Pickering, B. Garbarz, Scr. Metall. **21**, 249–254 (1987)
14. T. Gladman, I.D. Mcivor, F.B. Pickering, J. Iron Steel Inst. **210**, 916–930 (1972)
15. D.D. Chen, Y.C. Lin, Met. Mater. Int. **25**, 1246–1257 (2019)
16. S.I. Lee, S.Y. Lee, J. Han, B. Hwang, Mater. Sci. Eng. A **742**, 334–343 (2019)
17. C. Zener, J.H. Holloman, J. Appl. Phys. **15**, 22–32 (1944)
18. K.B. Kang, O. Kwon, W.B. Lee, C.G. Park, Scr. Mater. **36**, 1303–1308 (1997)
19. S.I. Lee, J. Lee, B. Hwang, Mater. Sci. Eng. A **758**, 56–59 (2019)
20. X. Deng, T. Fu, Z. Wang, G. Liu, G. Wang, R.D.K. Misra, Met. Mater. Int. **23**, 175–183 (2017)
21. H. Torkmani, S. Raygan, C.G. Mateo, J. Rassizadehghani, Y. Palizdar, Met. Mater. Int. **24**, 773–788 (2018)
22. P.C. Collins, S. Koduri, B. Welk, J. Tiley, H.L. Fraser, Metall. Mater. Trans. A **44**, 1441–1453 (2013)
23. G.Z. Quan, W.Q. Lv, Y.P. Mao, Y.W. Zhang, J. Zhou, Mater. Design **50**, 51–61 (2013)
24. Y. Sun, W. Zeng, Y. Han, X. Ma, Y. Zhao, P. Guo, G. Wang, M.S. Dargusch, Comput. Mater. Sci. **60**, 239–244 (2012)
25. W. Yu, M.Q. Li, J. Luo, S. Su, C. Li, Mater. Des. **31**, 3282–3288 (2010)
26. N.S. Reddy, J. Krishnaiah, H.B. Young, J.S. Lee, Comput. Mater. Sci. **84**, 120–126 (2015)
27. J. Kuisak, R. Kuziak, J. Mater. Process. Tech. **127**, 115–121 (2002)
28. G. Khalaj, H. yoozbashizadeh, A. Khodabandeh, A. Nazari, Neural Comput. Appl. **22**, 879–888 (2013)
29. B.E. O'Donnelly, R.L. Reuben, T.N. Baker, Met. Technol. **11**, 45–51 (1984)

30. D.E. Rumelhart, G.E. Hinton, R.J. Williams, Nature **323**, 533–536 (1986)
31. R.P. Lippmann, IEEE ASSP Mag. **4**, 4–22 (1987)
32. N. Hansen, Scr. Mater. **51**, 801–806 (2004)
33. K. Nakase, I.M. Bernstein, Metall. Mater. Trans. A **19**, 2819–2829 (1988)
34. C.M. Bae, C.S. Lee, W.J. Nam, Mater. Sci. Tech. **18**, 1317–1321 (2002)
35. C.M. Bae, W.J. Nam, Scr. Mater. **41**, 313–318 (1999)
36. W.D. Callister, D.G. Rethwisch, *Materials Science and Engineering*, 8th edn. (Wiley, New York, 2010)
37. T. Gladman, *The Physical Metallurgy of Microalloyed Steels* (The Institute of Materials, London, 1997)
38. O.P. Modi, N. Deshmukh, D.P. Mondal, A.K. Jha, A.H. Yegneswaran, H.K. Khaira, Mater. Charact. **46**, 347–352 (2001)
39. K. Matsuura, M. Tsukamoto, K. Watanabe, Acta Metall. **21**, 1033–1044 (1973)
40. S.S. Xu, Y. Zhao, X. Tong, H. Guo, L. Chen, L.W. Sun, M. Peng, M.J. Chen, D. Chen, Y. Cui, G.A. Sun, S.M. Peng, Z.W. Zhang, J. Alloy. Comp. **712**, 573–578 (2017)
41. T. Gladman, Mater. Sci. Tech. **15**, 30–36 (1999)
42. T. Takahashi, M. Nagumo, Trans. Jpn. Inst. Met. **11**, 113–119 (1970)
43. W.J. Nam, H.C. Choi, Mater Sci. Tech. **15**, 527–530 (1999)
44. C.C. Anya, T.N. Baker, Mater Sci. Eng. A **118**, 197–206 (1989)
45. Y.U. Heo, Y.Y. Song, S.J. Park, H.K.D.H. Bhadeshia, D.W. Suh, Metall. Mater. Trans. A **43**, 1731–1735 (2012)